International Journal of Remote Sensing
Vol. 30, No. 17, 10 September 2009, 4553–4565

Variations of chlorophyll-*a* in the northeastern Indian Ocean after the 2004 South Asian tsunami

DANLING TANG*†, HUI ZHAO†, B. SATYANARAYANA†‡§, GUANGMING ZHENG†, RAMESH P. SINGH¶, JIANHAI LV† and ZHONGZHENG YAN†

†Research Centre for Remote Sensing of Marine Ecology/Environment (RSMEE), LED, South China Sea Institute of Oceanology, Chinese Academy of Sciences, 164 West Xiangang Road, Guangzhou 510301, P. R. China

‡Institute of Oceanography, University Malaysia Terengganu, Mengabang Telipot, 21030 Kuala Terengganu, Malaysia

§Complexité et Dynamique des Systèmes Tropicaux, Département de Biologie des Organismes, Faculté des Sciences, Université libre de Bruxelles, ULB - Campus du Solbosch, B-1050 Bruxelles, Belgium

¶Department of Physics, Computational Science and Engineering, Schmidt College of Science, Chapman University, Orange, CA 92606, USA

(*Received 30 April 2007; in final form 7 August 2008*)

Analysis of satellite remote sensing data has revealed changes in distribution of chlorophyll-*a* (Chl-*a*) and sea surface temperature (SST) in the Indian Ocean during the South Asian tsunami in December 2004. Chl-*a* data derived from Moderate Resolution Imaging Spectroradiometer (MODIS) and Sea-viewing Wide Field-of-view Sensor (SeaWiFS) images were examined for the period from 1998 to 2005. Around the epicentre of the Sumatra earthquake, the Chl-*a* concentration was found to increase prior to the main event on 26 December 2004 and then decrease during the tsunami event, while a high SST (~30–31°C) was observed in and around the epicentral region. Chl-*a* concentrations in the coastal waters of the Southeast Asian countries were remarkably low during and after the tsunami. Similar but relatively small variations in Chl-*a* and SST were observed during the second earthquake on 28 March 2005. Analysis of Chl-*a*, SST, wind and upwelling water has provided information for understanding the changes in Chl-*a* concentration during the tsunami. A very large offshore phytoplankton bloom (~300 km^2) appeared to the southeast of Sri Lanka about 3 weeks after the tsunami; this might have been caused by a tropical storm that could be responsible for the enhancement of nutrients.

1. Introduction

On 26 December 2004, a strong earthquake off the northern Sumatra coast (Indonesia) produced the largest trans-oceanic tsunami in over 40 years, killing many people in the worst ever recorded tsunami and shifting the Andaman Nicobar islands (Hopkin 2005*a,b*, Jade *et al.* 2005, UNEP 2005, Gahalaut *et al.* 2006, Singh *et al.* 2007*a,b*). The epicentre of the earthquake that was located near latitude 3.3° N and longitude 95.95° E (figure 1), with a magnitude of 9.1 and a focal depth of 10 km,

*Corresponding author. Email: lingzistdl@126.com

International Journal of Remote Sensing
ISSN 0143-1161 print/ISSN 1366-5901 online © 2009 Taylor & Francis
http://www.tandf.co.uk/journals
DOI: 10.1080/01431160802603778

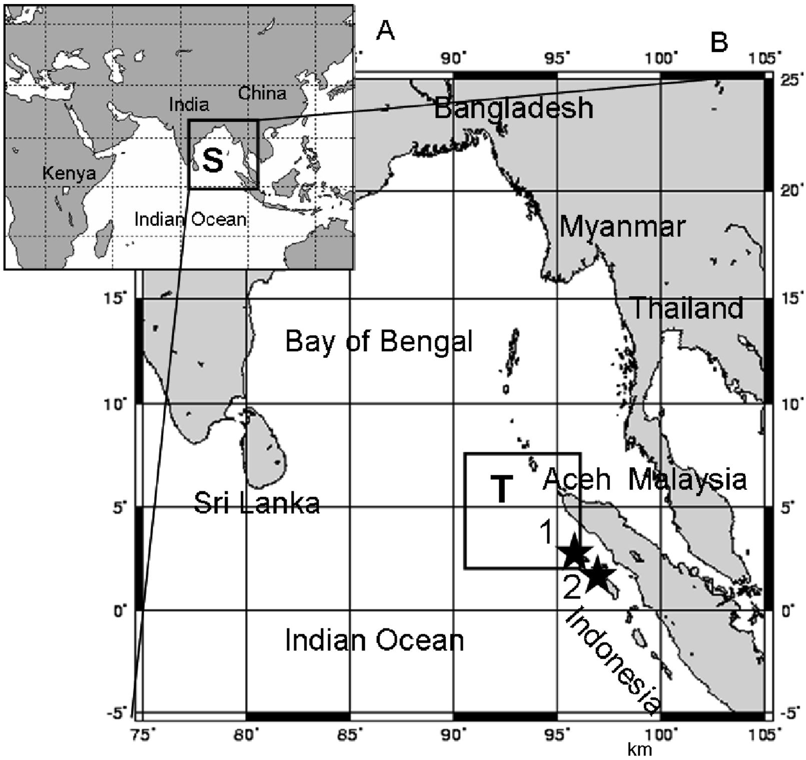

Figure 1. (*a*) Location of study area (box S); (*b*) study area. The epicentres of the earthquakes are marked with star/numbers - '1' for the disaster on 26 December 2004 and '2' for 28 March 2005. Box-T is the region for which time-series data of Chl-*a* and SST were examined. Provinces of Indonesia Labelled: Aceh, N.S.: North Sumatra, S.S: South Sumatra, W.S: West Sumatra, Riau and Jambi.

occurred on 26 December 2004 at 00:58:53 UTC (Coordinated Universal Time) (USGS 2004). People had not even recovered from the earlier shock when another strong earthquake (magnitude 8.7) occurred on 28 March 2005 (16:09:36 UTC) in the same region (2.07° N and 97.01° E) (USGS, 2005).

Tsunamis are caused by earthquakes, asteroid impacts, landslides, marine slides or volcanic eruptions under or near the oceans, also referred as 'tsunami seismic sea waves' (Bryant 2008, Dawson *et al.* 2004). During the 2004 South Asian tsunami, a trillion tonnes of water were displaced and driven along the southeast coasts of Asia by long and low-amplitude waves, at speeds of up to 900 km h^{-1} (Marris 2005*a*). Although the velocity of these waves slow down close to coastal regions due to the shallow water, the height of the waves increases tremendously (~30–50 m), destroying coastal regions with a devastating force (Cyranoski 2003). Such devastating waves caused damage to the buildings and vegetation along the coastal regions, destroying thousands of lives and damaging property worth millions of dollars.

Besides the numerous reports of the notable impact on human, social and economic sectors of society, the influences of tsunamis on ocean changes relating to sea level rise, seafloor pressure, biodiversity and biological production are also significant (Alverson 2005, Pearson 2005). Some studies have shown strong coupling between the lithosphere, hydrosphere and atmosphere associated with earthquakes, and as a result of this coupling, several types of earthquake precursory signals have been observed (Singh *et al*. 2002, 2007*a*,*b*, Dey and Singh 2003, 2004, Yan and Tang 2009). Attempts have been made to understand these precursory signals in order to obtain early warning information about an impending earthquake (Singh *et al*. 2007*a*,*b*). For example, an increase in suspended sediment after the Orissa super cyclone and the Sumatra tsunami has been reported (Kundu *et al*. 2001, Yan and Tang 2009). The bacterial population was found to occur at a maximum distance of 3 km in the Bay of Bengal beyond 10 km offshore after the tsunami (DOD 2005). A considerable amount of work has been focused on socioeconomics after the tsunami (UNEP 2005, Yanshuo 2005) while several studies are in progress on future warning systems (Cyranoski 2005, Jayaraman 2005, Marris 2005*b*), but very limited efforts have been made to study the impact of tsunamis on the phytoplankton ecosystem.

Using satellite data, we have made an attempt to address some of these concerns, mainly investigating chlorophyll-*a* (Chl-*a*) distribution, the fundamental element of primary production and a proxy of phytoplankton biomass. The main aim of the present study was to understand the changes occurring in the marine ecosystem after the earthquake/tsunami and the subsequent changes in the phytoplankton of the Indian Ocean.

2. Methods and data used

2.1 *Study area*

We considered the coastal area adjoining the Southeast Asian countries (–5° to 25° N and 75°–105° E) (box S, figure 1(*a*)) for an overall assessment of Chl-*a* concentration, sea surface temperature (SST) and wind variables in the Indian Ocean. For the evaluation of changes in ocean parameters (Chl-*a* and SST) associated with the Sumatra earthquake/tsunami, daily Chl-*a* concentration and 8-day composite SSTs were analysed over an area of 6° × 6° (2°–8° N and 90°–96° E) (box T in figure 1(*b*)) for the period 2002–2005.

2.2 *Remote sensing data and analysis*

2.2.1 Chlorophyll-*a* (Chl-*a*). The Chl-*a* data (level-3) derived from the Moderate Resolution Imaging Spectroradiometer (MODIS) (spatial resolution, 4 km) onboard the Aqua Earth Observing System (EOS) satellite (2002–2005) and Sea-viewing Wide Field-of-view Sensor (SeaWiFS) (1998–2005) are available from the National Aeronautics and Space Administration (NASA) Ocean Color Group (http://oceancolor.gsfc.nasa.gov). The data processing is carried out through $\log_{10}$ transformation and images are generated using MATLAB version 6.5 and GrADS (Grid Analysis and Display System) version 1.8.

2.2.2 Sea surface temperature (SST). SST data were obtained from the geophysical dataset of the observations collected by the Advanced Microwave Scanning Radiometer for EOS (AMSR-E) instrument onboard the NASA Aqua satellite. In the present study, we processed daily/monthly SST (ftp://ftp.discover-earth.org/sst/daily/amsre) with a 0.25° × 0.25° grid (1440 × 720 array), which is final product version 'v01'.

2.2.3 Sea surface wind (SSW). The daily wind data (level-3) of QuikSCAT (m s^{-1}, spatial resolution, 25 km) were taken from the Physical Oceanography Distributed Active Archive Centre (PO.DAAC) of the Jet Propulsion Laboratory, NASA (http://podaac.jpl.nasa.gov).

3. Results

3.1 *Variations in Chl-*a *distribution in the Indian Ocean*

MODIS images show spatial variations of Chl-*a* in the northern Indian Ocean (figure 2) during December–January, a small increase in Chl-*a* concentrations being clearly visible around the epicentre after the 26 December 2004 event. The Chl-*a* concentration was found to increase from the second week of December (figure 2(*b*)) until the first week (figure 2(*c*)) prior to the tsunami (26 December), and dispersed to a large area 3 weeks after the tsunami (figure 2(*d*)). Due to the cloud cover, the Chl-*a* distribution is not clearly seen but qualitatively the changes in distribution of Chl-*a* are clearly visible. Together with high Chl-*a* on the northeast of Sumatra Island (horizontal arrows in figures 2(*a*) and 2(*b*)), Chl-*a* is seen to decrease in the coastal waters adjacent to the Southeast Asian countries (India, Sri Lanka, Myanmar and Thailand; x and y regions in figure 2(*d*)), and increase in the offshore regions in the north of the Bay of Bengal abruptly after the tsunami (figure 2(*d*), see also figure 4(*Ac*)).

A large phytoplankton bloom (increase in Chl-*a* concentration) was observed southeast of Sri Lanka (Bay of Bengal) in January 2005, about 3 weeks after the tsunami (circle 1 in figure 2(*g*)), and the areal extent of the chlorophyll bloom was found to be larger than the Sri Lanka Island. The bloom appeared as a long narrow shape between Sri Lanka and Indonesia (figure 2(*h*)), a few weeks after the earthquake/tsunami event. A second bloom was also seen in the north of Sumatra Island (circle 2 in figure 2(*g*)), and later on this bloom was found to be dispersed in the surrounding region (figure 2(*h*)).

Figure 3 shows temporal changes in the phytoplankton bloom off Sri Lanka; the size of the bloom area appears to be almost the same size as Sri Lanka Island. The Chl-*a*

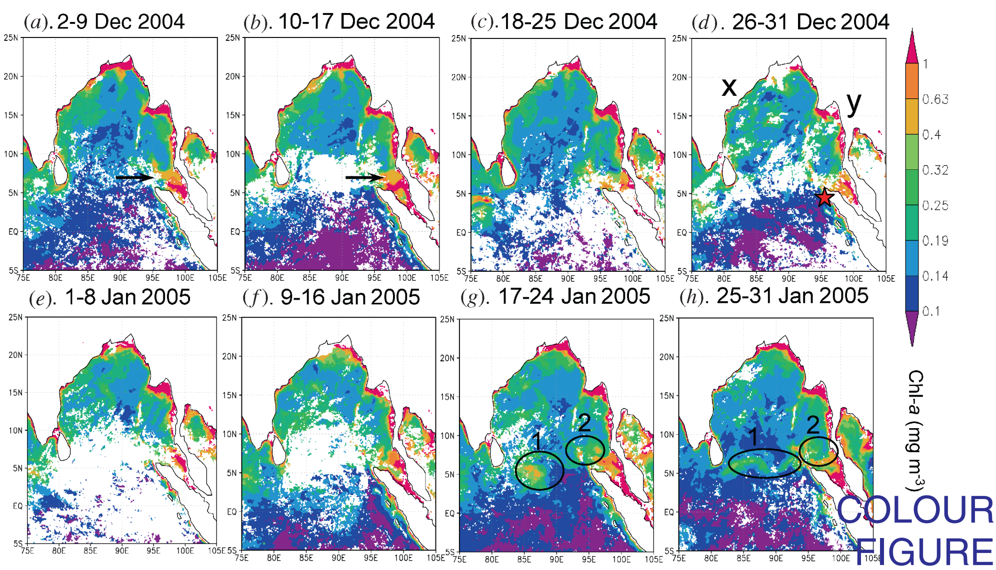

Figure 2. MODIS-derived Chl-*a* (mg m^{-3}) images (8-day compositions). The red star indicates the earthquake/tsunami on 26 December 2004. Arrows show high Chl-*a* to the northeast of Sumatra Island. Regions x and y denote changes in the coastal chlorophyll. Circles 1 and 2 indicate phytoplankton blooms. Interruption of the satellite coverage (white patches over the sea surface) is due to cloud cover.

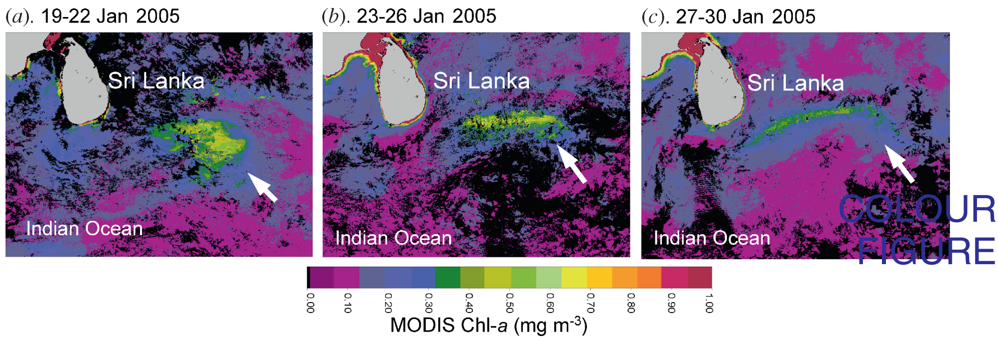

Figure 3. Large phytoplankton bloom in January 2005 (MODIS Chl-*a* images).

image for January 2005 clearly shows blooms at two locations (circles 1 and 2 in figure 4(*Ac*)); such blooms have not been observed in other years (figures 4(*Aa*) and 4(*Ab*)). It was difficult to ascertain the chlorophyll blooming close to the epicentre of main earthquake event of December 2004 because of the cloud cover. In view of this, daily and 8-day average Chl-*a* data were analysed (§3.4).

3.2 *SST and SSW*

3.2.1 Annual variability of SST. Figure 4(*B*) shows SST variations for the month of January from 2003 to 2005. The SST variations for January 2005 are seen to be lower

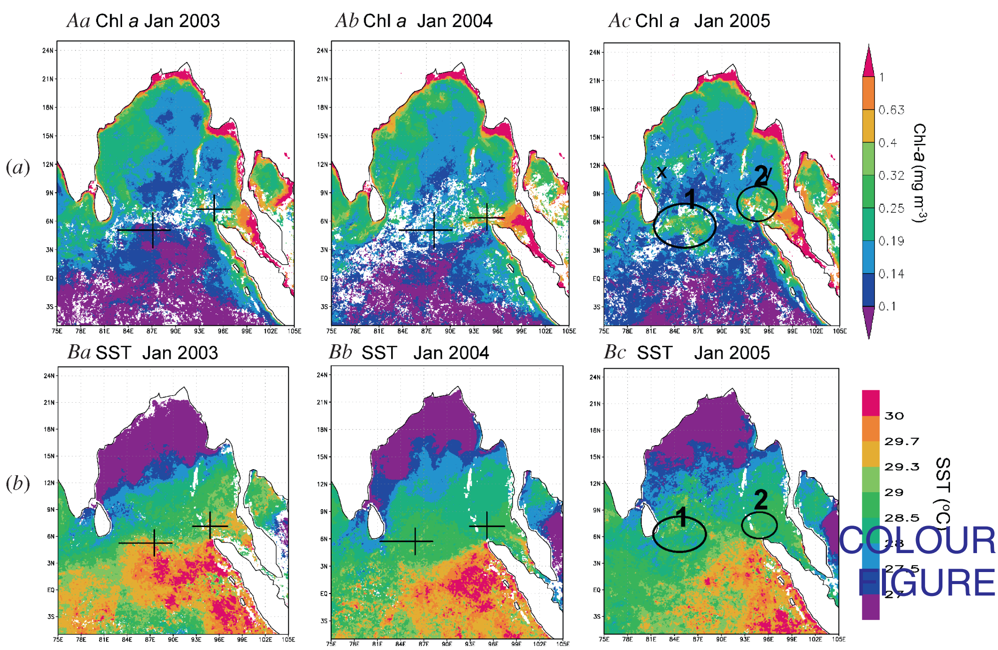

Figure 4. Monthly average images. Crosses marked within circles 1 and 2 show location of phytoplankton blooms in 2005. (*Aa–c*) MODIS-derived Chl-*a* (mg m^{-3}). (*Ba–c*) Sea surface temperature, SST (°C).

than those of 2003 and 2004. The low SST value around the epicentral region during January 2005 clearly reflects the effect of the tsunami. The low SST region corresponds to the higher Chl-*a* area after the main event of 26 December 2004, showing an inverse relationship between Chl-*a* and SST. Such conditions are favourable for chlorophyll blooming.

3.2.2 Variations in the daily SST. The daily SST distribution (figure 5(*A*)) shows a tendency to decrease by about 1°C over the southern part of the study area on 26 December 2004 (figure 5(*Ab*)), compared with 20 December (figure 5(*Aa*)), and this fall continues up to the end of the month (figure 5(*Ac*)). From 1 January 2005 (figure 5(*Ad*)), SST is found to increase and then return to normal levels (figure 5(*Aa*)). The SST was found to be significantly high (~30–31°C) on the west coast of northern Sumatra (close to the epicentre of the earthquake) (horizontal arrows in figures 5(*Aa*)–5(*Ad*)) with only a small variation (less than 0.5–1.0°C) on 26 December (horizontal arrow in figure 5(*Aa*)), and the areal extent of the high SST region reduced with time. Furthermore, low SST (27–28°C) was observed from the northeast to the southeast coast of India in the Bay of Bengal (downwards arrow in figure 5 (*Ac*)). The monthly average SST for the month of January in 2003–2005 (figure 4(*B*)) shows a relatively low temperature over the Indian Ocean after the tsunami (figure 4(*Bc*)) compared with other years (figures 4(*Ba*) and 4(*Bb*)), and also a low temperature at the location of phytoplankton blooms (circles 1 and 2 in figure 4(*Bc*)). The study area was mostly dominated by the northeastern winds due to the winter monsoon (November–February); the wind speed was 5.0 m s^{-1} on 20 December (figure 5(*Ba*)) and reached a maximum speed of ~10 m s^{-1} on 26 December (figure 5(*Bb*)) along the

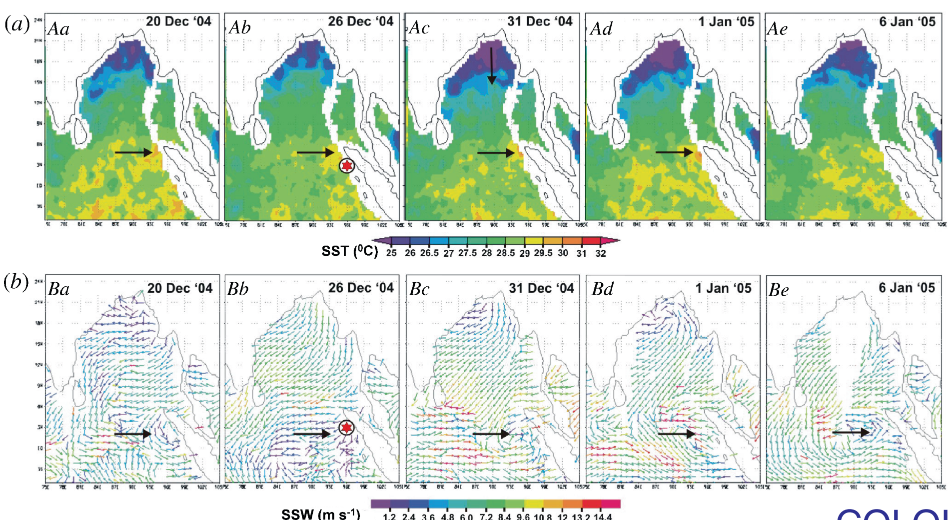

Figure 5. Time-series images for the tsunami period. The position of the earthquake/tsunami on 26 December 2004 is indicated by a red star. (*Aa–e*) Sea surface temperature, SST (°C). The arrow pointing down denotes the gradient of the lowering temperature from the northeast to the southeast coast of India in the Bay of Bengal; the horizontal arrows indicate the variation in temperature close to the epicentre of the earthquake. (*Ba–e*) Sea surface wind, SSW (m s^{-1}), showing wind speed and directions. A wind eddy in the vicinity of the earthquake is indicated by the horizontal arrows.

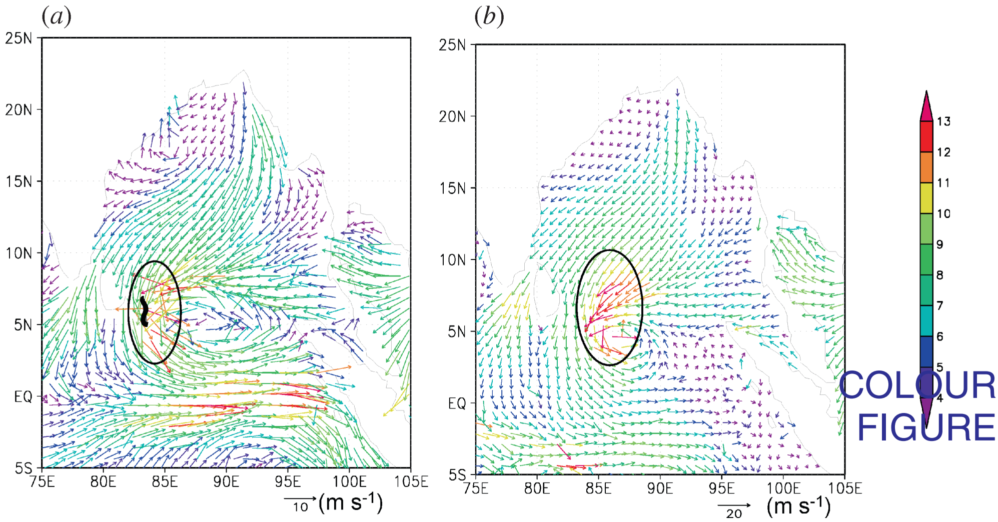

Figure 6. Tropical storm/depression and their tracks in January 2005. The short arrows show the wind speed (m s^{-1}). (*a*) 8–10 January 2005; (*b*) 14–16 January 2005.

southeast coast of India and Sri Lanka. The wind also changed its direction towards the east (down from the equator) and appeared as a large-scale cyclonic eddy in the vicinity of the earthquake (horizontal arrows in figures 5(*Ba*)–5(*Be*)).

3.2.3 SSW in January. A strong wind pattern ($>$ 12 m s^{-1}) (figure 6) was observed southeast of Sri Lanka and in mid-January 2005, in the shape of a cyclonic wind-strong region. According to hurricane data from the Joint Typhoon Warning Centre (JTWC) (available at http://weather.unisys.com), there was one tropical depression with a maximum speed (MS) of 13 m s^{-1} and one tropical storm with MS of 18 m s^{-1} over the above region during January, which had seldom occurred before in the month of January.

3.3 *Daily variation in Chl*-a

Daily variation in Chl-*a* concentration for the period October 2004–May 2005 is shown in figure 7(*a*). Chl-*a* concentration was found to increase prior to the eartquake (up to 0.3 mg m^{-3} on 22 December 2004) (1 in figure 7(*a*)), then decreased for 1 week during the tsunami, and increased again afterwards (2 in figure 7(*a*)). Similar variations were observed in March 2005, with two maximum peaks for Chl-*a* (3 and 4 in figure 5(*A*)), which are found to be associated with the second earthquake event of 28 March 2005. In general, Chl-*a* concentration showed an increasing trend during the period from December 2004 to March 2005 (line T in figure 7(*a*)).

The Chl-*a* (8-day averaged data) concentration was found to be low during October 2004–May 2005 compared with the other 3 years (2002–2005) (figure 7(*b*)). By contrast, high Chl-*a* concentration (arrow '26 Dec' in figure 7(*b*)) on 26 December 2004 shows an association with the earthquake event. Between mid-January and February, the Chl-*a* concentration was found to be a maximum (P in figure 7(*b*)) for both 2002–2003 and 2003–2004, but the Chl-*a* tendency to increase is found to be low from mid-January to February after the tsunami, compared with other years.

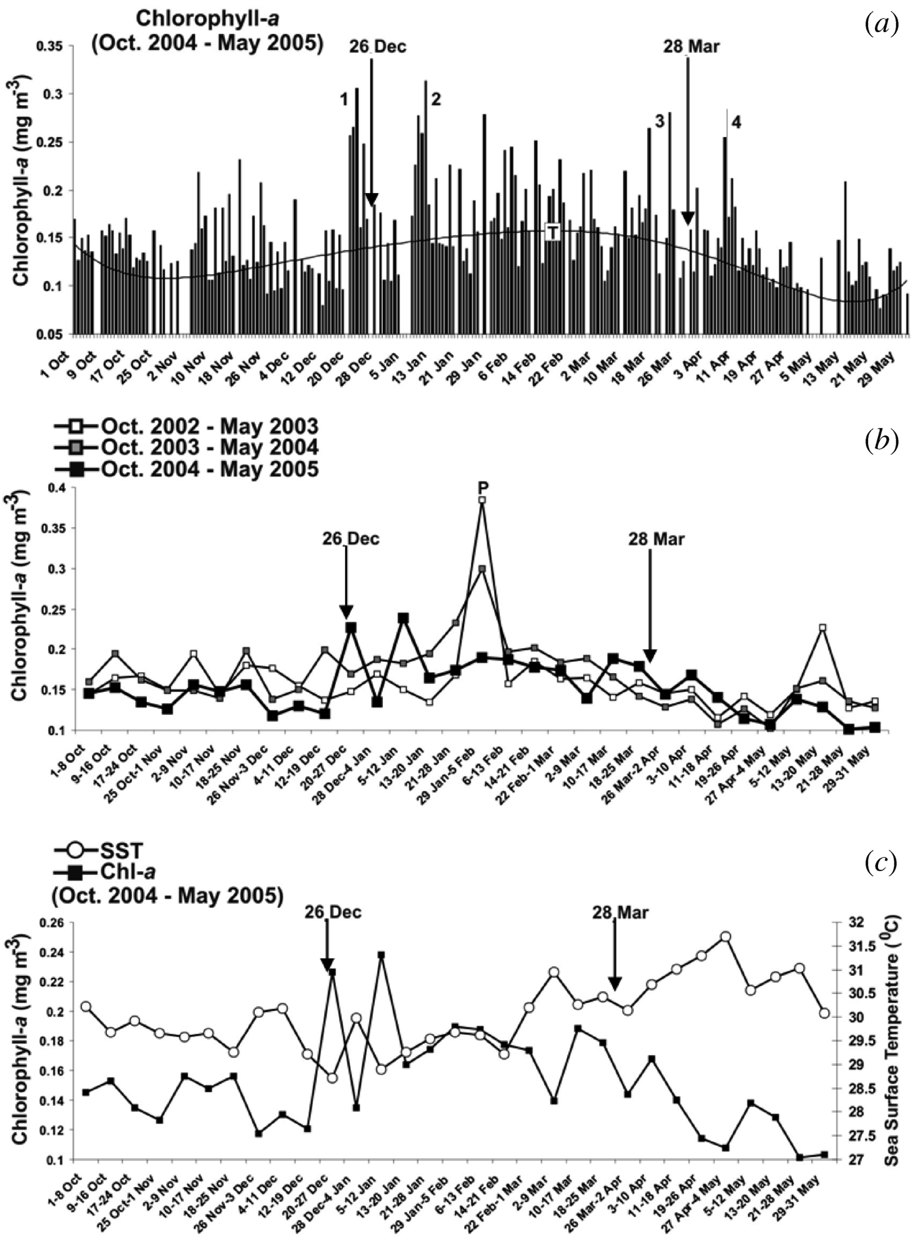

Figure 7. Time-series data averaged from box T (in figure 1(*b*)). (*a*) Daily Chl-*a* concentrations (MODIS). Line T shows the change trend. Numbers 1, 2, 3 and 4 indicate peaks of Chl-*a* concentration during the earthquakes. (*b*) Comparison of Chl-*a* (MODIS) over 3 years. P is the maximum Chl-*a* encountered between mid-January and February during 2002–2003 and 2003–2004. (*c*) Chl-*a* (MODIS) and SST relationship during October 2004–May 2005. The arrows indicate the dates of the earthquakes for all panels.

Figure 7(*c*) shows the Chl-*a* and SST (8-day averaged data) over the epicentral region (box T in figure 1(*b*)). SST was found to decrease from 30.1°C to 28.7°C during 4–27 December 2004 whereas Chl-*a* concentrations increased from 0.13 to 0.23 mg m^{-3},

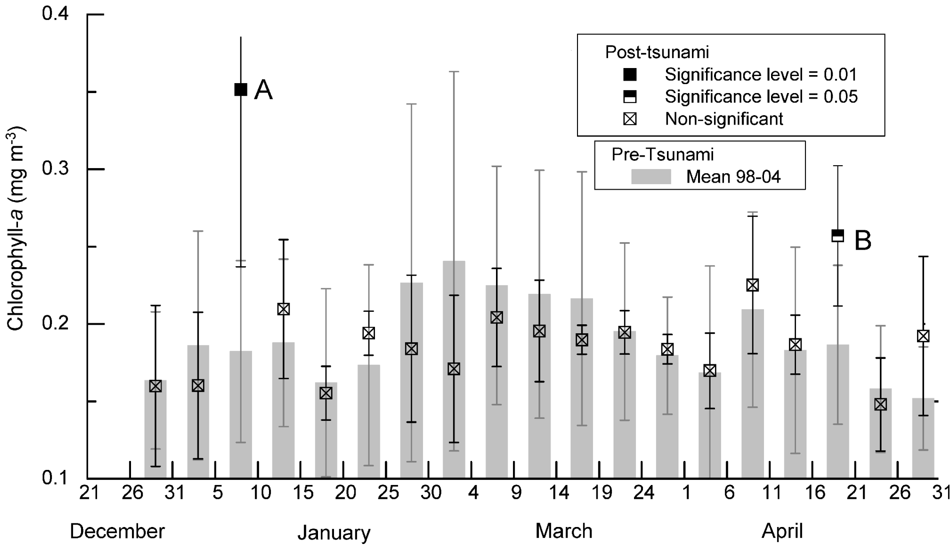

Figure 8. Statistical comparison of Chl-*a* (SeaWiFS) post-tsunami (26 December 2004–30 April 2005) and mean values pre-tsunami (26 December 1998–30 March 2004). Chl-*a* data were averaged spatially over the whole box T (in figure 1(*b*)).

clearly showing the impact of the earthquake/tsunami. Soon after the earthquake, SST was found to be high (29.9°C) from 28 December 2004 to 4 January 2005, whereas the Chl-*a* concentration had decreased to 0.13 mg m^{-3}.

With longer time data available from SeaWiFS, figure 8 shows a pronounced difference in Chl-*a* between the post-tsunami (December 2004–March 2005) and the pre-tsunami period for other years (December 1998–March 2004). Significant levels were computed using the '*t*' test using SPSS. We have used two-tailed significance, with equal variances assumed. Significant increases in Chl-*a* (figures 8(*a*) and 8(*b*)) were found up to about 2 weeks after the earthquake events of 24 December 2004 and 28 March 2005, respectively.

4. Discussion

4.1 *Oceanic conditions in the Bay of Bengal*

Spatial and temporal variability of Chl-*a* can be greatly influenced in large-scale disturbances by earthquakes, cyclones/hurricanes, extreme weather incidences in the upper oceans, and sudden changes in the thermal structure of the sea water (Kundu *et al*. 2001, Singh *et al*. 2002, 2007*a*,*b*, Tang *et al*. 2002, 2004, Chaturvedi and Narain 2003, Dey *et al*. 2004, Gautam *et al*. 2004, 2005, Zheng and Tang 2007). In the case of coastal earthquakes, the infrared (IR) temperature of the Earth's surface was found to change prior to the earthquake (Singh *et al*. 2007*a*,*b*).

In general, the Bay of Bengal shows higher primary productivity during the summer (May–September) than during the winter (November–February) monsoon because of the input of nutrients from rivers and the entrainment of sub-halocline layers through turbulent mixing (Ittekkot *et al*. 1991). However, high productivity in the onshore waters is still significant during the winter months due to Ekman transport towards the onshore (Naidu *et al.* 1999). Therefore, the coastal chlorophyll adjacent to the Southeast Asian countries (bordering the Bay of Bengal) is obviously a little high, whereas it was diluted and diffused by the giant waves just after the tsunami (x and y regions, figure 2(*d*)). In this context, a small increasing tendency of Chl-*a* (even after the tsunami) at the borders of Bangladesh, Myanmar and Thailand (y region in figures 2(*d*) and 4(*Ac*)) is perhaps due to propagation of the tsunami waves, which is much stronger in the east–west direction compared with the north–south direction (DOD 2005).

4.2 *Complexity among SST, SSW and Chl-*a

Light, temperature, nutrients and salinity are the important factors affecting the growth of phytoplankton (Singh *et al.* 2002, Dey and Singh 2003, 2004, Tang *et al.* 2003, 2004, 2006). The relationship between the ocean colour and SST is complex and depends on the season as well as geographic location. Earlier, Wiggert *et al.* (2001), Tang *et al.* (2002) and Yoder *et al.* (2002), and, more recently, Uz and Yodar (2004) have proposed the harmony between these two factors, where the relationship depends very much on the process of mixing or upwelling. However, the SST in the epicentral region was also found to be high, with the temperature ranging between 30°C and 31°C (horizontal arrows in figures 5(*Aa*)–5(*Ad*)), which may be due to the release of thermal energy (Dey and Singh 2003, Gautam *et al.* 2004, Singh *et al.* 2007*a*,*b*). A lowering of SST by about 1°C on the day of the tsunami was also observed in the surroundings of the Andaman and Nicobar Islands region (DOD 2005).

4.3 *Phytoplankton blooms associated with nutrient increases*

The increase in coastal nutrients due to the tsunami (Yan and Tang 2008) may have stimulated phytoplankton growth along the coastal water. The bloom observed to the north of Aceh Province (Indonesia) (circle 2 in figures 2(*g*) and 4(*Ac*)) is also probably due to an increase in coastal nutrients or enhanced upwelling or vertical mixing.

The large offshore bloom southeast of Sri Lanka (figure 6) that appeared in January 2005 may be due to tropical storms that took place 2–3 weeks after the tsunami. The strong winds during the storm can induce vertical mixing or upwelling, leading to high concentrations of nutrients at the surface (Tang *et al.* 2002, 2006, Zheng and Tang 2007, Zhao *et al.* 2008). A detailed study is needed to understand the processes associated with chlorophyll blooming due to the tsunami and tropical storms and also to provide a quantitative evaluation of chlorophyll blooming.

5. Summary

The present study shows the changes in Chl-*a* distribution in the local regions around Sumatra, South Asian waters (the Bay of Bengal and the Andaman Sea) and at coastal areas of the Southeast Asian countries during the 2004 tsunami. The mechanism of changes of Chl-*a* and SST in the Indian Ocean during and after the tsunami are not yet well understood. Based on the present results, we propose a strategy (figure 9) of the possible influences of the undersea earthquake and tsunami.

In the vicinity of the earthquake, the enhanced Chl-*a* concentration and the corresponding decrease in SST produces favourable conditions for the upwelling and vertical mixing of water due to disturbances associated with the tsunami (phases 1–4 in figure 9). High waves during the tsunami wash the land surface and bring nutrients to the coastal

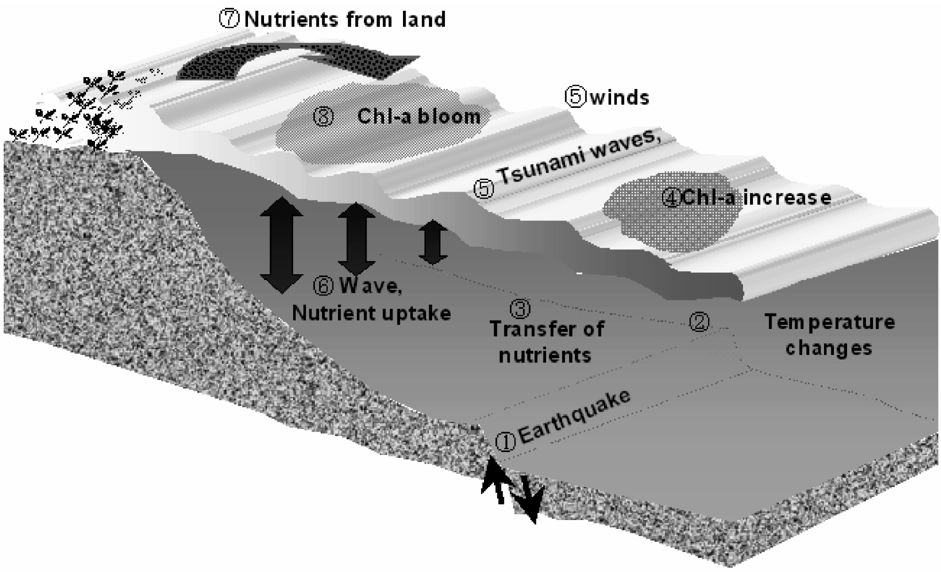

Figure 9. Schematic representation showing the ecological consequences of the tsunamis.

waters (phases 5–7 in figure 9), and as a result phytoplankton blooms (phase 4 in figure 9) are likely to occur. The growth of phytoplankton/Chl-*a* in the vicinity of the earthquake prior to the tsunami was found to be associated with strong winds and changes in the ocean. A large offshore phytoplankton bloom to the southeast of Sri Lanka (phase 9 in figure 9) was attributed to strong tropical winds, which supports the enhancement of nutrients due to vertical mixing (phase 8 in figure 9).

Acknowledgements

The present work was supported by research grants from (1) the National Natural Science Foundation of China (NSFC40576053 and 40811140533) and the Natural Science Foundation of Guangdong Province, China (2008 Partnership program for typhoon research); and (2) the Chinese Academy of Sciences (CAS) (LYQY200701) and the CAS/SAFEA International Partnership Program for Creative Research Teams awarded to Professor DanLing Tang; and (3) a post-doctoral fellowship of CAS awarded to Dr Satyanarayana (No. 2005037619). We are grateful to the Editor and the anonymous referees for their comments/suggestions that have helped to improve the original version of the manuscript.

References

Alverson, K., 2005, Watching over the world's oceans. *Nature*, **434**, pp. 19–20.

Bryant, E., 2008, *Tsunami: The Underrated Hazard*. (Berlin: Springer), p. 342.

Chaturvedi, N. and Narain, A., 2003, Chlorophyll distribution pattern in the Arabian Sea: seasonal and regional variability, as observed from SeaWiFS data. *International Journal of Remote Sensing*, **24**, pp. 511–518.

Cyranoski, D., 2003, Earthquake makes waves for tsunami models. *Nature*, **425**, p. 649.

Cyranoski, D., 2005, Solo efforts hamper tsunami warning system. *Nature*, **433**, p. 343.

Dawson, A.G., Lockett, P. and Shi, S., 2004, Tsunami hazards in Europe. *Environment International*, **30**, pp. 577–585.

Dey, S., Sarkar, S. and Singh, R.P., 2004, Anomalous changes in column water vapour after Gujarat earthquake. *Advances in Space Research*, **33**, pp. 274–278.

Dey, S. and Singh, R.P., 2003, Surface latent heat flux as an earthquake precursor. *Natural Hazards and Earth System Sciences*, **3**, pp. 1–7.

Dey, S. and Singh, R.P., 2004, Comparison of chlorophyll distributions in the northeastern Arabian Sea and southern Bay of Bengal using IRS-P4 Ocean Color Monitor Data. *Remote Sensing of Environment*, **85**, pp. 424–428.

DOD, 2005, *Preliminary Assessment of Impact of Tsunami in Selected Coastal Areas of India* (Chennai, India: Department of Ocean Development, ICMAM Project Directorate).

Gahalaut, V.K., Nagarajan, B., Catherine, J.K. and Kumar, S., 2006, Constraints on 2004 Sumatra–Andaman earthquake rupture from GPS measurements in Andaman–Nicobar Islands. *Earth and Planetary Science Letters*, **242**, pp. 365–374.

Gautam, R., Cervone, G., Singh, R.P. and Kafatos, M., 2005, Characteristics of meteorological parameters associated with Hurricane Isabel. *Geophysical Research Letters*, **32**, L04801, doi:10.1029/2004GL021559.

Gautam, R., Singh, R.P., Cervone, G. and Kafatos, M., 2004, Changes in ocean properties associated with Hurricane Isabel. *International Journal of Remote Sensing*, **26**, pp. 643–649.

Hopkin, W., 2005*a*, Triple slip of tectonic plates caused seafloor surge. *Nature*, **433**, p. 3.

Hopkin, M., 2005*b*, Indonesia spared tsunami as disaster quake strikes. *Nature*, **434**, p. 547.

Ittekkot, V., Nair, R.R., Honjo, S., Ramaswamy, V., Barstch, M., Manganini, S. and Desai, B.N., 1991, Enhanced particle fluxes in Bay of Bengal induced by injection of fresh water. *Nature*, **351**, pp. 385–387.

Jade, S., Ananda, M.B., Dileep Kumar, P. and Banerjee, S., 2005, Co-seismic and post-seismic displacements in Andaman and Nicobar Islands from GPS measurements. *Current Science*, **88**, pp. 1980–1984.

Jayaraman, K.S., 2005, India pledges to fund alert system in wake of disaster. *Nature*, **433**, p. 5.

Kundu, S.N., Mohapatra, S., Sahoo, A.K. and Singh, R.P., 2001, Change analysis using IRS-P4 OCM data after the Orissa super cyclone. *International Journal of Remote Sensing*, **22**, pp. 1383–1389.

Marris, E., 2005*a*, Inadequate warning system left Asia at the mercy of tsunami. *Nature*, **433**, pp. 3–5.

Marris, E., 2005*b*, Indian Ocean fault line poses threat of future earthquakes. *Nature*, **433**, p. 183.

Naidu, P.D., Ramesh Kumar, M.R. and Ramesh Babu, V., 1999, Time and space variations of monsoonal upwelling along the west and east coasts of India. *Continental Shelf Research*, **19**, pp. 559–572.

Pearson, H., 2005, Scientists seek action to fix Asia's ravaged ecosystems. *Nature*, **433**, p. 94.

Singh, R.P., Bhoi, S. and Sahoo, A.K., 2002, Changes observed on land and ocean after Gujarat earthquake 26 January 2001 using IRS data. *International Journal of Remote Sensing*, **23**, pp. 3123–3128.

Singh, R.P., Cervone, G., Kafatos, M., Prasad, A.K., Sahoo, A.K., Sun, D., Tang, D.L. and Yang, R., 2007*a*, Multi-sensor studies of the Sumatra earthquake and tsunami of 26 December 2004. *International Journal of Remote Sensing*, **28**, pp. 2885–2896.

Singh, R.P., Cervone, G., Singh, V.P. and Kafatos, M., 2007*b*, Generic precursors to coastal earthquakes: inferences from Denali fault earthquake. *Tectonophysics*, **431**, pp. 231–240.

Tang, D.L., Kawamura, H., Lee, M.A. and Dien, T.V., 2003, Seasonal and spatial distribution of chlorophyll-a concentrations and water conditions in the Gulf of Tonkin, South China Sea. *Remote Journal of Geophysical Research*, **85**, pp. 475–483.

Tang, D.L., Kawamura, H. and Luis, A.J., 2002, Short-term variability of phytoplankton blooms associated with a cold eddy on the north-western Arabian Sea. *Remote Sensing of Environment*, **81**, pp. 81–89.

Tang, D.L., Kawamura, H., Nhu, H.D. and Takahashi, W., 2004, Remote sensing oceanography of a harmful algal bloom (HAB) off the coast of southeastern Vietnam. *Journal of Geophysical Research*, **109**, C03014, doi:10.1029/2003jc002045.

Tang, D.L., Kawamura, H., Shi, P., Takahashi, W., Shimada, T., Sakaida, F. and Isoguchi, O., 2006, Seasonal phytoplankton blooms associated with monsoonal influences and coastal environments in the sea areas either side of the Indochina Peninsula. *Journal of Geophysical Research*, **111**, G01010, doi:10.1029/2005JG000050.

UNEP, 2005, *After the Tsunami: Rapid Environmental Assessment* (Naribi, Kenya: United Nations Environment Programme).

USGS, 2004, *United States Geological Survey – Earthquake Hazards Program*. Available online at: http://earthquake.usgs.gov/eqinthenews/2004/usslav.

Uz, B.M. and Yoder, J.A., 2004, High frequency and mesoscale variability in SeaWiFS chlorophyll imagery and its relation to other remotely sensed oceanographic variables. *Deep Sea Research*, **51**, pp. 1001–1017.

Wiggert, J.D., Murtugudde, R.G. and McClain, C.R., 2001, Processes controlling inter-annual variations in wintertime (northeast monsoon) primary productivity in the central Arabian Sea. *Deep Sea Research*, **49**, pp. 2319–2343.

Yan, Z.Z. and Tang, D.L., 2009, Changes in suspended sediments associated with 2004 Indian Ocean tsunami. *Advances in Space Research*, **43**, pp. 89–95.

Yanshuo, N., 2005, Outpouring of aid. News report. *Beijing Review*, **48**, pp. 12–14.

Yoder, J.A., Schollaert, S.E. and O'Reilly, J.E., 2002, Climatological phytoplankton chlorophyll and sea-surface temperature patterns in continental shelf and slope waters off the northeast U.S. coast. *Limnology and Oceanography*, **47**, pp. 672–682.

Zhao H., Tang, D.L. and Wang, Y.Q., 2008, Comparison of phytoplankton blooms triggered by two typhoons with different intensities and translation speeds in the South China Sea. *Marine Ecology Progress Series*, **365**, pp. 57–65.

Zheng, G.M. and Tang, D.L., 2007, Offshore and nearshore chlorophyll increases induced by typhoon and typhoon rain. *Marine Ecology Progress Series*, **333**, pp. 61–74.